in the polymer, since for every chlorine atom added to the polymer, one hydrogen atom is lost. Second, more hydrogen is consumed in producing HCl. That is, presumably more HCl is formed from the polymer during pyrolysis as the chlorine level increases. The HCl pyrolyzate yield as a function of polymer chlorine level has apparently not been the subject of careful study, however. A third possible explanation would be that more hydrogen remains in the polymer residue as char as the chlorine level increases. This is probably not a factor, since chars are generally very deficient in hydrogen.

While PVC itself produces little char during thermal decomposition, addition of chlorine to the polymer results in a steady increase in char residue.[6,18] This implies that cross-linking mechanisms not significant in PVC become important as more chlorine is added to the polymer. These mechanisms may involve intermolecular HCl elimination, Diels–Alder reactions, and various free radical processes.

These preliminary results suggest that Py–MS with computerized statistical analysis holds considerable potential for characterizing the composition and studying thermal decomposition mechanisms in chlorine-containing polymers. Further studies are in progress that should help to elucidate the thermal decomposition behavior of CPVC in more detail.

Acknowledgment. Appreciation is expressed to The BFGoodrich Co. for support of this work. W. Windig and A. M. Harper (University of Utah) assisted with the computerized statistical analysis, and W. H. McClennen (University of Utah) performed the Curie-point Py–MS experiments. I. Sockis and R. E. Harris (The BFGoodrich Co.) assisted with the Py–GC and Py–GC–MS experiments. Helpful discussions with E. D. Dickens, Jr., G. S. Huvard, R. A. Komoroski, W. J. Kroenke, M. H. Lehr, and R. G. Parker (The BFGoodrich Co.) are appreciated. S. A. Liebman (Chemical Data Systems, Inc.) is also acknowledged for encouraging us to work on this project.

Registry No. Chlorobenzene, 108-90-7.

References and Notes

(1) Berticat, P. *J. Chim. Phys.* **1967**, *64*, 887.
(2) Berticat, P. *Rev. Gen. Caout. Plast.* **1971**, *48*, 1361.
(3) Tsuge, S.; Okumoto, T.; Takeuchi, T. *Macromolecules* **1969**, *2*, 277.
(4) Liebman, S. A.; Reuwer, J. F., Jr.; Gollatz, K. A.; Nauman, C. D. *J. Polym. Sci., Part A-1* **1971**, *9*, 1823.
(5) Liebman, S. A.; Ahlstrom, D. H.; Quinn, E. J.; Geigley, A. G.; Meluskey, J. T. *J. Polym Sci., Part A-1* **1971**, *9*, 1921.
(6) Quinn, E. J.; Ahlstrom, D. H.; Liebman, S. A. *Polym. Prepr. Am. Chem. Soc., Div. Polym. Chem.* **1973**, *14* (2), 1022.
(7) Liebman, S. A.; Levy, E. J. *J. Chromatogr. Sci.* **1983**, *21*, 1.
(8) Lukáš, R.; Světlý, J.; Kolínský, M. *J. Polym. Sci., Polym. Chem. Ed.* **1981**, *19*, 295.
(9) Keller, F.; Hösselbarth, B. *Faserforsch. Textiltech.* **1978**, *29*, 152.
(10) Komoroski, R. A.; Parker, R. G.; Lehr, M. H. *Macromolecules* **1982**, *15*, 844.
(11) Harper, A. M.; Meuzelaar, H. L. C.; Given, P. H.; Pope, D. L.; Metcalf, G. S. "Analytical Pyrolysis"; Voorhees, K. J., Ed.; Butterworth: Woburn, MA, 1983.
(12) Nie, N. H.; Hull, C. H.; Jenkins, J. G.; Steinbrenner, K.; Bent, W. H. "Statistical Package for the Social Sciences", 2nd ed.; McGraw-Hill: New York, 1975.
(13) Windig, W.; Meuzelaar, H. L. C.; Haws, B. A.; Campbell, W. F.; Asay, K. H. *J. Anal. Appl. Pyrol.*, in press.
(14) O'Mara, M. M. *Pure Appl. Chem.* **1977**, *49*, 649.
(15) Starnes, W. H., Jr.; Edelson, D. *Macromolecules* **1979**, *12*, 797.
(16) Lattimer, R. P.; Kroenke, W. J. *J. Appl. Polym. Sci.* **1982**, *27*, 1355.
(17) Lattimer, R. P., unpublished results.
(18) Dickens, E. D., Jr., The BFGoodrich Co., private communication.

Study of the Low-Frequency Acoustic Modes of Oriented Poly(ethylene) with a Multipass Fabry–Perot Interferometer

Q.-L. Liu and C. H. Wang*

Department of Chemistry, University of Utah, Salt Lake City, Utah 84112.
Received December 7, 1982

ABSTRACT: The low-frequency spectra of high-density polycrystalline poly(ethylene) films are studied with a Fabry–Perot interferometer. The sound velocities and associated elastic constants are determined as a function of stretch ratio (R_s). In contrast to the results of other polymer films, the spectral line associated with the longitudinal acoustic phonon propagating along the stretch axis shows increased broadening as the film is gradually stretched. For films stretched to $R_s = 7.0$ or above, the longitudinal acoustic phonon spectrum broadens considerably and finally merges with the background noise. This unusual feature is attributed to the interaction between the localized LAM associated with the lamellae stems and the long-wavelength longitudinal acoustic wave propagating along the orientation axis. This hypothesis is corroborated by the observation of the angular independence of the low-frequency spectrum of a high-pressure crystallized poly(ethylene) with large lamellar thickness (≈7000 Å). The effects of annealing and quenching on the Brillouin frequencies of the oriented film are also investigated.

Introduction

The poly(ethylene) (PE) chain has the simplest repeat unit of all synthetic high polymers. The structural simplicity of this polymer has promoted many theoretical and experimental studies that have the aim of characterizing its physical properties. One area of current research interest is the vibrational spectroscopy of the PE chain in the solid state. Calculations of the normal modes of vibration in the PE crystal[1,2] have shown that the interchain interactions between adjacent chains in the unit cell affect the vibrational modes of the crystal significantly. The low-frequency acoustic modes are strongly affected by the crystal field and thus deserve to be studied in more detail.

A considerable amount of information regarding the morphology of semicrystalline PE has been obtained from the Raman scattering study of the longitudinal acoustic mode, or LAM. In the crystalline *n*-paraffins[3] and in PE single crystals,[4-6] the frequency of the LAM is found to be inversely proportional to the straight chain length. In semicrystalline PE, the microstructure is composed of

0024-9297/83/2216-1900$01.50/0

crystalline and amorphous regions. The LAM is found to be confined to the crystalline region that is bounded between the amorphous phases.[5,7-12] The frequency of the LAM is limited by the lamellar stem length in the crystalline region. The lamellar thickness of ordinary semicrystalline PE is of the order of 200 Å, and the LAM frequency that appears in the Raman spectrum lies between 6 and 50 cm^{-1}. At larger lamellar thickness, the LAM spectrum cannot be obtained by the conventional Raman spectrometer. In order to study LAM at lower frequencies from samples of large lamellar thickness, a Fabry–Perot interferometer is needed for spectral analysis.

Related to LAM spectroscopy is Brillouin scattering. Brillouin light scattering is generally considered to be associated with the scattering of thermally generated acoustic phonons in a given medium. The acoustic phonon interacts with and shifts the frequency of the incident light in the scattering event. The velocity of sound measured from the Brillouin frequency shift is given by

$$V_s = \frac{f_B \lambda_i}{(n_i^2 + n_s^2 - 2n_i n_s \cos\theta)^{1/2}} \quad (1)$$

where f_B is the frequency shift, λ_i is the wavelength in vaccuo of the incident light, n_i and n_s are, respectively, indices of refraction of the incident and scattering light waves in their respective directions of propagation, and θ is the scattering angle. The Brillouin shifts in solid-state polymers are typically on the order of 0.3 cm^{-1}, which corresponds to a sonic frequency of about 10 GHz. In the experiments reported here, the wavelength of the thermally induced acoustic phonon from which scattering occurs is about 3500 Å. In ordinary high-density PE, the average crystallite dimension along the c axis is on the order of 250 Å,[5] and the phonon wavelength spans several crystalline and amorphous regions. The long-wavelength acoustic phonon is thus affected by the composite crystalline–amorphous microstructure.

In general, a Fabry–Perot interferometer is used in the Brillouin scattering experiment, and a Raman spectrometer (equipped with a double-grating monochromator) is used in the LAM measurement. However, when the lamellar thickness of the semicrystalline polymer increases, the LAM frequency may decrease to the spectral region where the conventional Raman spectrometer becomes unuseable. For example, the lamellar thickness of the high-pressure crystallized poly(ethylene) may increase to at least 2000 Å, and the LAM frequency from such a sample will be of the order of 1 cm^{-1}. The detection of such a low LAM frequency will require a Fabry–Perot interferometer. Thus, in the Brillouin scattering experiment of a high-pressure crystallized PE, spectral lines from both the long-wavelength acoustic waves and LAM may simultaneously appear.

However, it should be emphasized that even though LAM is referred to as the longitudinal acoustic mode, the nature of LAM is different from the long-wavelength acoustic mode involved in the usual Brillouin scattering experiment. As pointed out above, LAM arises from the crystalline lamellae and as such it is a localized intramolecular mode; the frequency of such a mode is independent of the scattering angle. On the other hand, the long-wavelength acoustic phonons are collective, involving polymer segments in both the crystalline and the amorphous regions; therefore, the acoustic phonon frequency depends on the scattering angle (cf. eq 1). This important difference may be used to differentiate LAM bands from spectral lines that arise from the long-wavelength acoustic phonons.

Table I
Density (ρ) and Crystalline Fraction (x) of the PE Films at Various Draw Ratios (R_s)

R_s	R_s	ρ/(g cm^{-1})	x
	1	0.960	0.745
	2.2	0.960	0.745
	3.2	0.961	0.753
	4.3	0.960	0.745
	5.2	0.966	0.780
	6.5	0.968	0.794
	7.0	0.972	0.821

Both solid-state extrusion and uniaxial stretching produce samples with uniaxially symmetric morphology. In uniaxial symmetry, the z symmetry axis is taken to be the orientiation axis and is perpendicular to the x and y axes. The sonic properties measured along the x and y axes are equivalent, and the x–y plane is isotropic.[13-17] Thus, in a uniaxially oriented polymer solid with sound propagating along the symmetry axis, there are one pure longitudinal mode and two degenerate pure transverse modes. For propagation directions away from a symmetry axis, one of the transverse modes and the longitudinal mode are mixed, forming the quasi-longitudinal (QL) mode and the quasi-transverse (QT) mode. In the polymer samples studied so far, only the pure longitudinal modes, the QL and QT modes, scatter strongly and appear prominently in the Brillouin spectra of uniaxially oriented polycrystalline polymers. Pure transverse modes have been found to scatter weakly in most of these polymers.

While the Brillouin spectrum of the unoriented PE film appears more or less the same as that of the other polymer films,[14] the Brillouin spectrum of the oriented semicrystalline PE shows quite a different behavior from what is observed for other polymers. Not only is the transverse component found to scatter more strongly in oriented PE, but also the longitudinal mode propagating along the stretch direction is found to broaden considerably. In the highly oriented state, the pure longitudinal mode that propagates along the stretch (z) axis broadens out completely and does not appear in the Brillouin spectrum. The same result is found in a high-pressure unoriented crystallized poly(ethylene) (HPCPE) with large lamellar thickness (≈7000 Å). In such a sample, the low-frequency (0–50 GHz) sample displays only the LAM spectrum;[18] the Brillouin spectrum from the longitudinal acoustic phonon is not found. This paper reports these findings and also makes an attempt to interpret these unusual results.

Experimental Section

The poly(ethylene) film samples were prepared from high-density Marlex no. 6003 (density equal to 0.963 g/cm^3), supplied by the Phillips Petroleum Co. The polymer sample was pressed into sheets under pressure between heated plates (the plate temperature was 205 °C). The sheets were held in the press for 20 min before quenching in water for 2 h. The temperature of the water was kept, respectively, at 0, 10, 20, 30, 40, and 50 °C. This allowed the study of the effect of the quenching temperature.

A series of films with draw ratios of 2.2, 3.2, 4.3, 5.2, 6.5, and 7.0 were prepared by stretching strips cut from the sheets submerged in a water bath at 90 °C with a stretching rack. The draw ratios were measured from the separation of the marks on the films. All films appear translucent.

The density of the films was determined by using a gradient density column tube filled with water–isopropyl alcohol. From the measured density value, the crystalline fraction of the films was determined through the expression

$$x = (\rho_c/\rho)(\rho - \rho_a)/(\rho_c - \rho_a) \quad (2)$$

where ρ_c (=1.002 g/cm^3) and ρ_a (=0.855 g/cm^3)[12] are the crystalline and amorphous density, respectively. In Table I, one notes that x increases slightly with increasing R_s. Brillouin scattering spectra

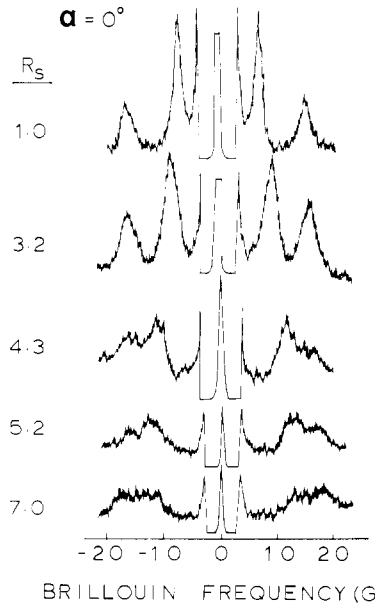

Figure 1. Brillouin spectra of films stretched to different stretch ratio (R_s) taken with the scattering geometry such that the scattering vector **q** is along the direction of the stretch.

were obtained with an optical apparatus similar to that reported previously.[13] The spectrometer consisted of a piezoelectricaly scanned Fabry–Perot interferometer operated in five passes. The free spectral range (FSR) was set at 30 or 20 GHz, depending upon the situation. The overall finesse of the optical system was kept between 50 and 55. The incident radiation at about 4880 Å was from an Ar^+ laser equipped with an etalon for single-mode operation. Approximately 300 mW of the laser power was used to obtain the film spectra. The laser light was vertically polarized, and the scattered polarization was analyzed with a Glan–Thompson prism. All spectra reported were polarized (VV).

To monitor the velocities of sound waves propagating in various directions in the film surface, the sample was mounted on a goniometer that showed the precise rotation angle of the sample in the scattering plane. A detailed description of this method was given previously in ref 13.

The low-frequency light scattering spectrum in the 0–50 GHz region of a piece of high-pressure crystallized poly(ethylene) (HPCPE) sample was also recorded with the five-pass Fabry–Perot interferometer at three scattering angles (30°, 90°, and 170°). The HPCPE sample was prepared by Dr. W. Frank (Universitat Ulm, West Germany) and given to us by Dr. John Rabolt (IBM Research Laboratories, San Jose, CA.).

Results and Discussion

The Brillouin spectra of films stretched to different stretch ratio (R_s) taken at $\alpha = 0°$ (α being the angle between **q** associated with the scattering from the incident beam and the orientation axis) are shown in Figure 1. At low draw ratio, two peaks are clearly evident. The low-frequency peak corresponds to scattering of the incident beam by the longitudinal acoustic phonon. The high-frequency peak corresponds to scattering of the internally reflected beam inside the film. The phonon propagating direction associated with this spectral line is perpendicular to the z axis.[17] Figure 1 shows the effect of stretching on the spectrum of the longitudinal phonon that propagates parallel to the orientation axis of the films. In the unoriented film, the longitudinal line is narrow, but as the film is drawn, the longitudinal line broadens progressively, and in the highly drawn film, it becomes so broad as to nearly merge with the base line noise. Further, one notes that as the film is stretched, the spectral peaks shift to higher frequencies, which is to be expected from the increase in the alignment of the polymer chains with respect to the z axis.[16]

Table II
Relations of $(\delta\epsilon^{-1})_{ij}$ to the Components of the Strain Tensor in a Uniaxial System

$$(\delta\epsilon^{-1})_{xx} = P_{11}S_{xx} + P_{12}S_{yy} + P_{13}S_{zz}$$
$$(\delta\epsilon^{-1})_{xy} = P_{66}S_{xy}$$
$$(\delta\epsilon^{-1})_{xz} = P_{44}S_{xz}$$
$$(\delta\epsilon^{-1})_{yy} = P_{12}S_{xx} + P_{11}S_{yy} + P_{13}S_{zz}$$
$$(\delta\epsilon^{-1})_{yz} = P_{44}S_{yz}$$
$$(\delta\epsilon^{-1})_{zz} = P_{13}S_{xx} + P_{13}S_{yy} + P_{33}S_{zz}$$

The intensity of the Brillouin spectrum is determined by the mean square fluctuation of the dielectric constant tensor $\delta\epsilon$. In the present experiment, the incident and scattering radiations are both polarized in the plane of the polymer film; the VV component of the $\delta\epsilon$ tensor is related to the $\delta\epsilon^{-1}$ tensor by

$$\delta\epsilon_{VV} = -\epsilon_{Vi}^{0}\epsilon_{Vj}^{0}(\delta\epsilon^{-1})_{ij} \quad (3)$$

where i and j refer to the optical axes of the film. (The summation convention with repeated indices indicating summation over the index will be implied throughout this paper.) We assume that the optical axes coincide with the laboratory axes (i.e., the orientation axis is z, the y axis is perpendicular to the film surface, and the x axis lies in the plane of the film), and we write $\delta\epsilon_{VV}$ as

$$\delta\epsilon_{VV} = -[\epsilon_1^2 \cos^2\alpha(\delta\epsilon^{-1})_{xx} - 2\epsilon_\perp\epsilon_\parallel \cos\alpha \sin\alpha(\delta\epsilon^{-1})_{xz} + \epsilon_\parallel^2 \sin^2\alpha(\delta\epsilon^{-1})_{zz}] \quad (4)$$

where $\epsilon_\parallel$ and $\epsilon_\perp$ are the dielectric constants parallel and perpendicular to the orientation (z) axis, respectively.

If Pockel's law is applicable, then $\delta\epsilon^{-1}$ is related to the strain tensor **S** by

$$(\delta\epsilon^{-1})_{ij} = P_{ijkl}S_{kl} \quad (5)$$

where P_{ijkl} are the photoelastic constants. Explicit expressions for $(\delta\epsilon^{-1})_{ij}$ in a uniaxial system are given in Table II. If the relaxation effect is neglected, then the strain tensor **S** and the stress tensor **T** can be written as

$$T_{ij} = C_{ijkl}S_{kl} \quad (6)$$

where C_{ijkl} are the elastic constants.

In accordance with eq 4 and Table II, the expression of $\delta\epsilon_{VV}$ for **q** parallel to the z axis (or $\alpha = 0$) can be written as

$$\delta\epsilon_{VV} = -\epsilon_\perp^2 P_{13}S_{zz} \quad (7)$$

Since only the longitudinal acoustic phonon contributes to S_{zz}, one expects to observe one line corresponding to the phonon with the frequency given by $(C_{33}/\rho)^{1/2}$ in the $\alpha = 0°$ scattering spectrum. Similarly, the expression of $\delta\epsilon_{VV}$ for **q** parallel to the x axis (or $\alpha = \pi/2$) is given by

$$\delta\epsilon_{VV} = -\epsilon_\parallel^2 P_{13}S_{xx} \quad (8)$$

Thus only the longitudinal phonon with the frequency given by $(C_{11}/\rho)^{1/2}$ will appear in the $\alpha = \pi/2$ spectrum. For $0° < \alpha < \pi/2$, scatterings from both the longitudinal and the transverse phonons are expected to be present.

Equations 7 and 8 provide the basic background for analyzing the change of the Brillouin spectrum as a function of α. Shown in Figure 2 are the Brillouin spectra obtained for the $R_s = 7.0$ film at various α angles. The spectra were obtained with the film mounted on the goniometer so that by rotating the film, the angle between **q** and the stretch axis could be varied.

One notes that a sharp spectral line is present in the $\alpha = \pi/2$ spectrum. According to eq 8, this spectral line is

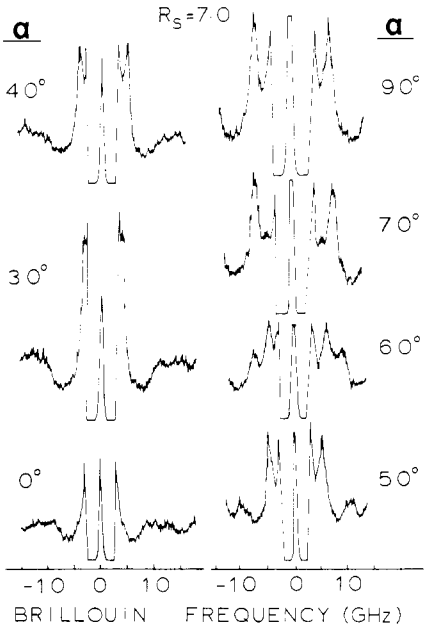

Figure 2. Brillouin spectra obtained for the R_s = 7.0 film at various α angles.

associated with the longitudinal acoustic phonon, and its intensity is proportional to $\epsilon_{\parallel}{}^4 P_{13}{}^2 \langle |S_{xx}(\mathbf{q})|^2 \rangle$, where the angular brackets denote the ensemble average. The frequency of the longitudinal acoustic phonon is reflected by the value of the elastic constant C_{11} and the density ρ of the stretched film.

At $\alpha = 70°$, the sharp peak moves to a higher frequency, accompanied by the development of a new feature at the lower frequency. At $\alpha = 60°$, the new feature becomes quite prominent and the high-frequency component broadens considerably. These two spectral lines correspond to the QT and QL modes. At $\alpha = 50°$, the QL mode moves to higher frequency and displays further broadening. The QT mode, which has acquired considerable intensity, moves to lower frequency. As the angle α further decreases, the QT mode gradually moves inward and merges with the intense Rayleigh line. At the same time, the QL mode further broadens and becomes a part of a broad spectral background. At $\alpha = 0°$, only a very broad feature is present; there is no trace of the longitudinal component.

The unusual feature displayed in Figure 2 is the absence of the expected sharp longitudinal acoustic phonon in the $\alpha = 0°$ spectrum. When α is changed from 90° to 0°, the spectrum associated with the longitudinal phonon moves out to high frequency accompanied by gradual broadening. This result contrasts with those found in other polymer films in which the $\alpha = 0°$ ($\mathbf{q}$ parallel to the z axis) spectrum is dominated by a sharp spectral line associated with the pure longitudinal phonon.

As pointed out above, the PE microstructure has been described as a lamellar composite of crystalline and amorphous regions. The effects of stretching and extrusion on this microstructure have been studied by other techniques. Upon stretching, the amorphous chains are drawn into parallel alignment with the orientation axis, and the crystalline regions are oriented so that the crystal c axis is aligned with the orientation axis. Samples that are extruded to high area reduction ratios, e.g., >12×, have nearly 100% orientation of both the crystalline and amorphous regions. The degree of orientation for the crystalline region in the film is also high, although less than that produced by extrusion. These stretching and extrusion processes produce uniaxially symmetric samples, but the microstructure produced by each process may be different.[16]

The unusual feature observed in the Brillouin spectra of oriented PE is presumably related to changes in the polymer microstructure as the film is drawn. Previous studies in PE indicate that stretching or extrusion induces disruption of the microstructure and a reduction in the regularity of the lamellar texture.[5,6] But, if the broadening were due to the gross disruption of the microstructure, we would expect the QL and QT modes to be affected in a similar manner; however, as shown in Figure 2, the line width of the QT mode does not appear to be affected significantly by stretching. In fact, Brillouin measurements of an extruded sample (R_s = 36) at $\alpha = 0°$ show the presence of a narrow spectral line,[22] the frequency of which is identified as associated with the pure *transverse* acoustic phonon with $C_{44} = 1.59 \times 10^{10}$ dyn/cm^2. The longitudinal spectral line is absent in the $\alpha = 0°$ spectrum of the extruded rod.[22] Thus, it is unlikely that the gross disruption of the microstructure in PE is the source causing the line broadening of the longitudinal phonon propagating along the orientation axis.

The line broadening in PE may be caused by the interaction of the long-wavelength longitudinal acoustic mode with the LAM modes of the straight-chain segments as induced by stretching. In the isolated chain, vibrational analysis shows that the ν_5 dispersion curve contains CCC bending and CC stretching and intersects the Brillouin zone center ($\delta = 0°$, δ being the vibrational phase between adjacent methylene groups of the PE chain) at zero frequency, corresponding to a pure translation parallel to the chain axis.[22] The ν_9 dispersion curve includes modes that involve torsional vibration about the CC bonds. When intermolecular interactions in the crystal are considered, mixing between ν_5 and ν_9 occurs, giving rise to the lattice vibration of the crystal. Since there are two molecules in the unit cell, each dispersion curve splits at the zone center.[2] Thus $\nu_5{}^a$ and $\nu_5{}^b$ (at $\delta = 0°$) are the rotational modes; $\nu_9{}^a$ becomes the translational lattice mode while $\nu_9{}^b$ becomes the longitudinal acoustic branch in the vicinity of $\delta = 0°$.

Since the frequency of $\nu_9{}^b$ is a function of δ, it is reasonable to expect that the highly oriented PE film may contain segments with such chain lengths that give rise to a frequency distribution with considerable spectral power density at the frequency region of the longitudinal acoustic phonon. Furthermore, since highly deformed PE samples contain a large number of straight chains with variable chain length, such structural defects in the sample will also result in considerable spectral power density in the acoustic phonon region. Considering the above, it is not unreasonable to state that the present result shows the existence of coupling between the longitudinal acoustic phonon and the LAM. The coupling of LAM with the longitudinal acoustic phonon is reasonable because LAM belongs to the A_g symmetry species, which is identical with the stress tensor along the stretched axis (S_{zz}). As a result, the energy of the acoustic phonon that propagates along the z axis will interact with the intramolecular LAM and is then dissipated through the crystalline lamellae. This mechanism is assumed to be the cause of the line broadening.

To support this hypothesis, we have carried out interferometric measurements of a semicrystalline HPCPE sample. The straight-chain length of this sample is over 7000 Å,[18] and as such, the LAM frequency is estimated to occur in the 15–30-GHz region, which corresponds to the frequency range of the longitudinal acoustic phonon of highly oriented PE films. Thus, if coupling is present

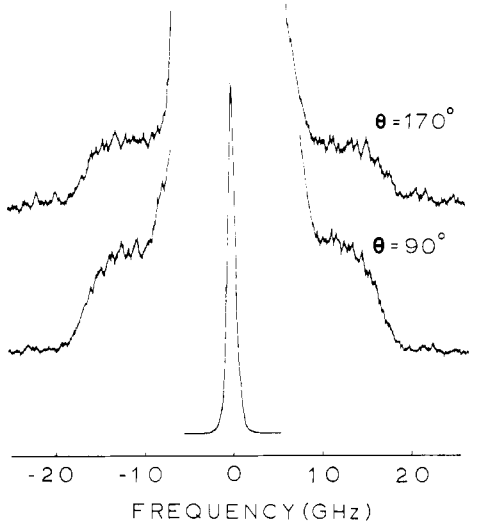

Figure 3. Low-frequency spectra of high-pressure crystallized poly(ethylene) rod taken at three scattering angles.

between the LAM and the longitudinal acoustic phonon, a broad spectrum similar to that observed in the $\alpha = 0°$ spectrum of the highly oriented film will be manifested in the low-frequency region. Further, since the LAM frequency is a localized mode, if the scattering is dominated by the LAM, the low-frequency spectrum of the HPCPE sample will not depend on the scattering angle, contrary to the q-dependent Brillouin spectrum.

Shown in Figure 3 are the low-frequency spectra fo HPCPE taken at two scattering angles. One notes that the distinctive Brillouin spectral feature is absent from the spectrum; furthermore, while the spectral intensity shows some variation with the scattering angle, the broad feature on both sides of the intense Rayleigh peak is nearly independent of the scattering angle. Overall, the spectrum is similar to the $\alpha = 0°$ spectrum in Figure 2. Thus, the result obtained for the low-frequency spectrum of HPCPE is consistent with that observed in the highly oriented film and the extruded PE rod.[22] It is thus a definite result that in highly oriented PE films, the longitudinal acoustic phonon propagation along the orientation axis is highly damped.

In the birefringent medium, the hypersonic velocity V_s and the Brillouin frequency f_B are related by eq 1. In PE, the birefringence is less than 10^{-3} even in the highly oriented film. Thus, within the accuracy of the experiment (2% in V_s), we set $n_i = n_s$. Furthermore, for the scattering geometry with the film surface bisecting the angle (90°) between the incident and scattered beams, eq 1 simplifies to[17]

$$V_s = f_B \lambda_i / 2^{1/2} \tag{9}$$

The sound velocity contours for the unstretched (R_s = 1.0) and the highly stretched films (R_s = 7.0) are plotted as a function of the angle α in Figure 4. In the unstretched film, the sound velocity is isotropic across the film surface. In the R_s = 7.0 film, both QT and QL phonons are present. Moreover, considerable anisotropy in the sound velocities is clearly seen. The longitudinal sound velocity across the orientation axis is considerably less than that along the orientation axis. The transverse velocity appears to be maximum at $\alpha \simeq 45°$. In Figure 5, the sound velocities V_s are plotted as a function of R_s at various α. The data presented in Figures 4 and 5 are obtained by rotating the film surface about the azimuthal axis, keeping the plane of the film at 45° with respect to the incident and the scattered beams. Rotation of the film changes the direction of the phonon propagation vector $\mathbf{q}$ in the plane of the sample, and, hence, the sound velocity in the various directions in the stretched film can be determined. One notes that, despite somewhat larger experimental uncertainty due to line broadening, the sound velocity measured at $\alpha = 0°$ does not increase above $R_s \simeq 7.0$. This indicates that by stretching, the sound velocity of the drawn semicrystalline PE does not reach the crystalline value.[25,26]

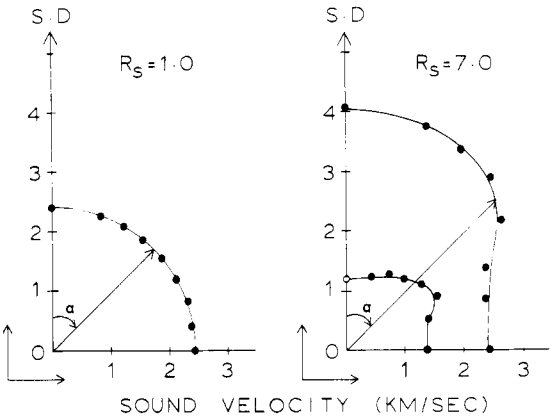

Figure 4. Sound velocity contours for the unstretched and the stretched films (R_s = 7.0) plotted as a function of α. The transverse velocity at $\alpha = 0°$ is a calculated value as indicated by the empty circle.

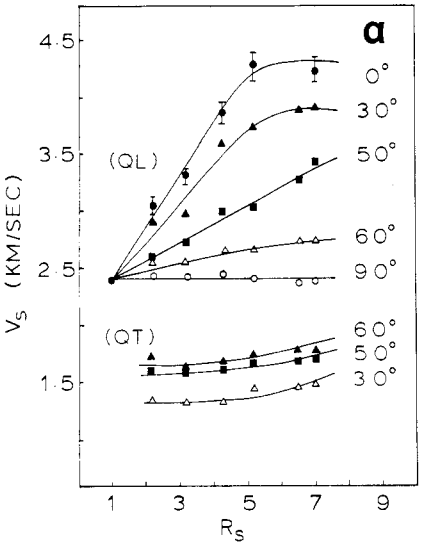

Figure 5. Longitudinal and transverse sound velocities at various α as a function of stretch ratio.

A deformation process, such as stretching or extrusion, changes the symmetry of an oriented isotropic solid to cylindrical (uniaxial) symmetry. The elastic constant tensor of a solid with cylindrical symmetry has the form

$$C_{ijkl} = \begin{bmatrix} C_{11} & C_{12} & C_{13} & & & \\ C_{12} & C_{11} & C_{13} & 0 & 0 & \\ C_{13} & C_{13} & C_{33} & & & \\ & & & C_{44} & & \\ & 0 & & & C_{44} & \\ & & & & & C_{66} \end{bmatrix} \tag{10}$$

where $C_{66} = {}^1/_2 (C_{11} - C_{12})$. The contracted subscript notation of Voigt is used for C_{ijkl} (and for the photoelastic constant P_{ijkl}.

For the sound wave propagating in the plane of the film (the x–z plane), the velocities of the QL and QT acoustic

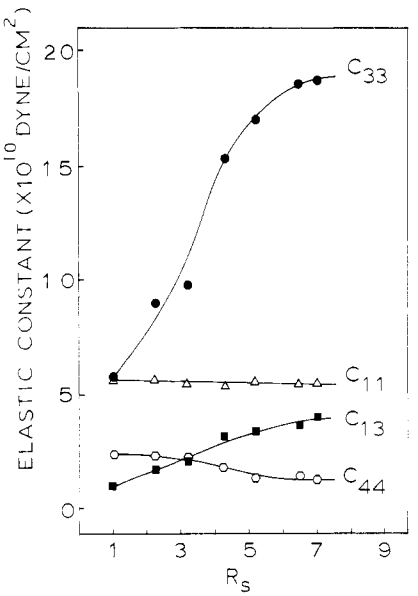

Figure 6. Elastic constants C_{11}, C_{33}, and C_{44} of poly(ethylene) films plotted as a function of stretch ratio.

waves are related to the elastic constants C_{11}, C_{33}, C_{44}, and C_{13} by the equation

$$V_{\pm}^2 = \frac{1}{2\rho}((C_{11}l_x^2 + C_{33}l_z^2 + C_{44}) \pm [(C_{11}l_x^2 + C_{33}l_z^2 + C_{44})^2 - 4\{(C_{11}l_x^2 + C_{44}l_z^2)(C_{33}l_z^2 + C_{44}l_x^2) - l_x^2l_z^2(C_{13} + C_{44})\}]^{1/2}) \quad (11)$$

where the V_+ and V_- correspond to the QL and QT velocities, respectively, $l_x = \sin\alpha$, and $l_z = \cos\alpha$. With the help of a least-squares fitting program developed previously,[14] we fit the sound velocity data (presented in part in Figure 4) to eq 11 and obtain the elastic constants C_{11}, C_{33}, C_{44}, and C_{13} for the film at a given stretch ratio. The set of elastic constants obtained from the fit are plotted as a function of the draw ratio in Figure 6. Like other polymer films, the largest change in the elastic constant appears in C_{33}, which increases rapidly with increasing R_s until $R_s = 7.0$. Above $R_s = 7.0$, C_{33} only increases slightly. At $R_s = 7.0$, the value of C_{33} is equal to 18.8×10^{10} dyn/cm^2, which is about a factor of 3.4 times larger than the value of the unstretched film. The value of C_{11} remains more or less unchanged (equal to 5.52×10^{10} dyn/cm^2). The elastic constant C_{13} increases from 1.03×10^{10} dyn/cm^2 at $R_s = 1.0$ to 4.09×10^{10} dyn/cm^2 at $R_s = 7.0$, whereas the value of C_{44} decreases from 2.36×10^{10} dyn/cm^2 at $R_s = 1.0$ to 1.40×10^{10} dyn/cm^2 at $R_s = 7.0$.

The variation behavior of the elastic constants of the poly(ethylene) film due to stretch differs significantly from that found in the poly(propylene) (PP) film. In poly(propylene), the change of C_{33} with R_s is linear up to $R_s = 7.0$, whereas the change of C_{33} with R_s in poly(ethylene) is nonlinear. Another important difference in PE is the decrease of C_{44} when R_s is increased. In PP and other polymer films, C_{44} does not change with increasing R_s. The increase of C_{13} with increasing R_s in the PE film is also significantly larger than that found in other polymer films that so far have been investigated in this laboratory.

The elastic constant C_{13} is a measure of the effect of the normal strain (S_{zz}) when a normal stress (T_{xx}) is applied in the direction perpendicular to the stretch. An increase in C_{13} with deformation suggests that the stress on the segments over the dimension of the acoustic wavelength becomes increasingly larger as the polymer is stretched.[16]

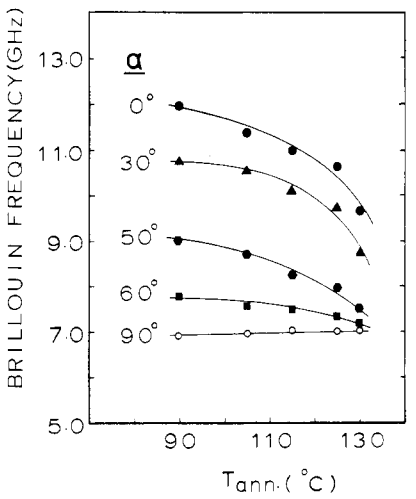

Figure 7. Effect of annealing on the acoustic phonon frequencies for the film stretched to $R_s = 5.2$.

The elastic constant C_{44} is a measurement of the efficiency of the storage of the shear strain energy when the film is subject to the shear stress (T_{yz}). Thus, stretching apparently decreases the capacity of the PE film to store the shear strain energy.

The elastic constant calculated along the chain axis in all *all-trans*-PE chain as determined from the LAM frequencies of the *n*-alkanes is about equal to 300×10^{10} dyn/cm.[26] This is, however, more than 1 order of magnitude higher than the C_{33} value of the highest stretched film. The difference in the two types of C_{33} value arises from the fact that the wavelength of the acoustic phonon monitored by Brillouin scattering is considerably greater than the lamellar thickness so that several crystalline and amorphous regions are spanned by the acoustic wave. thus, the elastic constants obtained from Brillouin scattering reflect the mechanical response of the composite microscopic structure of the film, which is considerably softer than the oriented chains in the lamellae. Although stretching orients and extends the PE chains, local crystallization induced by stretching does not increase the size of the lamellae to the microscopic dimension. This is probably due to the disruption of the microscopic structure when the PE film is stretched to a great extent. As a result, the elastic constant C_{33} of the semicrystalline PE film reaches a plateau value after it is stretched to some R_s value.

Studies of the effect of annealing on the Brillouin spectrum of the oriented film are expected to provide additional information about the mechanism that leads to the change of the Brillouin spectra of PE films. Shown in Figure 7 are the longitudinal ($\alpha = 0°$ and 90°) and quasi-longitudinal ($0° < \alpha < 90°$) acoustic phonon frequencies as a function of the annealing temperature for the $R_s = 5.2$ film. In the annealing experiment, a film that was initially stretched to $R_s = 5.2$ at 90 °C was submerged in an oil bath at 105 °C for 2 h, while held at constant length. The film was then removed from the bath and cooled to room temperature before the Brillouin spectra at various α angles were measured. This process was repeated with the annealing temperature set at 115, 125, and 130 °C. Above 130 °C, the film softened and no measurement was carried out above this temperature.

In Figure 7, one notes that annealing has no effect on the frequency of the spectrum taken at $\alpha = 90°$. However, for α less than 90°, the frequency decreases with the increase of the annealing temperature. The frequency of the $\alpha = 0°$ spectrum displays the largest decrease.

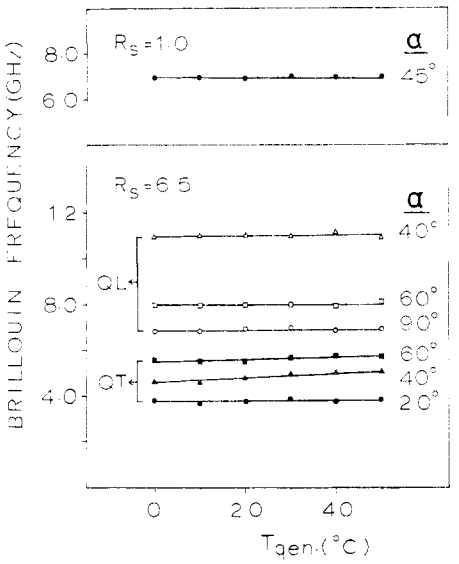

Figure 8. Negligible effect of quenching temperature on the Brillouin frequencies of the unoriented (R_s = 1.0) and the oriented film (R_s = 6.5).

Two effects are present when the PE film is annealed. One effect is the reduction of the chain orientation, leading to the decrease of C_{33}. This effect should result in decreasing the frequency of the $\alpha = 0°$ spectrum, as the $\alpha = 0°$ spectrum is directly associated with C_{33}. The $\alpha = 90°$ spectrum is associated with the elastic constant C_{11} and is not significantly affected by the change of the chain orientation (cf. Figure 6). The other effect introduced by annealing is involved with the increase in the density and the lamellar thickness.[27] Since the increase in the lamellar thickness enhances the rigidity and the increase in the density decreases the frequency, the second effect introduced by annealing is not expected to result in any significant frequency change. This is supported by the insensitive frequency variation of the $\alpha = 90°$ spectrum with annealing and indicates that the effect on the frequency introduced by these two opposing factors cancel each other out. Thus the frequency decrease found in the $0° \leq \alpha < \pi/2$ spectrum is due mainly to the orientation loss introduced by annealing. However, the fact that the frequency of the $\alpha = 0°$ spectrum for the film annealed at 130 °C remains higher than the value of the unoriented film (which is equal approximately to the frequency of the $\alpha = 90°$ spectrum) indicates the presence of residual orientation in the amorphous region which is still not annealed away. The residual orientation is presumably associated with the tie molecules joining the lateral faces of lamellae in spherulites. These tie molecules are expected to be greatly affected by stretching, and since annealing increases the lamellar thickness, the orientation of the tie molecules cannot easily be annealed away.

The quenching temperature of the compressed hot film plays an important role in the growth of lamellae. The effect of quenching temperature on the Brillouin frequencies of the unoriented (R_s = 1.0) film and the oriented film (R_s = 6.5) is shown in Figure 8. While the Brillouin frequency of the QT acoustic mode seems to increase slightly with increasing quenching temperature, the effect on the QL acoustic mode is negligible. Since the quenching temperature affects the crystallinity of PE film by affecting the fold length of the lamellae, the negligibly small change of the Brillouin frequencies of both the oriented and unoriented films with quenching temperature indicates that the Brillouin scattering spectra of PE films are affected mainly by the structural change in the amorphous phase and not by the detail of chain fold. While quenching or annealing are known to change crystallinity of PE, it appears that the Brillouin frequency is only affected significantly by the orientational state of the amorphous chains.

Acknowledgment. We acknowledge the Office of Naval Research and the NSF Polymers Program (Grant No. DMR 79-12457) for providing financial support for this research. We also thank Dr. John F. Rabolt and IBM for providing us with a high-pressure crystallized poly(ethylene) sample.

Registry No. Poly(ethylene) (homopolymer), 9002-88-4.

References and Notes

(1) M. Tasumi and T. Shimanouchi, *J. Chem. Phys.*, **43**, 4, 1245 (1965).
(2) M. Tasumi and S. Krimm, *J. Chem. Phys.*, **46**, 2, 755 (1967).
(3) R. F. Schaufele and T. Shimanouchi, *J. Chem. Phys.*, **47**, 3605 (1967).
(4) M. J. Folkes, A. Keller, J. Steiny, P. L. Coggin, G. V. Fraser, and P. J. Hendra, *Colloid Polym. Sci.*, **253**, 354 (1975).
(5) H. C. Olf, A. Peterlin, and W. L. Peticolas, *J. Polym. Sci., Polym. Phys. Ed.*, **12**, 359 (1974).
(6) J. L. Koenig and D. L. Tabb, *J. Macromol. Sci. Phys.*, **39** (1), 141 (1974).
(7) G. V. Fraser, P. J. Hendra, M. E. A. Cudby, and H. A. Willis, *J. Mater. Sci.*, **9**, 1270 (1974).
(8) G. Capacio, M. A. Wilding, and I. M. Ward, *J. Polym. Sci., Polym. Phys. Ed.*, **19**, 1489 (1981).
(9) S. L. Hsu and S. Krimm, *J. Appl. Phys.*, **47** (10), 4265 (1976).
(10) R. C. Snyder and J. Scherer, *J. Polym. Sci., Polym. Phys. Ed.*, **18**, 421 (1980).
(11) R. C. Snyder, *J. Polym. Sci., Polym. Phys. Ed.*, **16**, 1593 (1978).
(12) K.-J. Choi, J.-E. Sprasiell, and J. L. White, *J. Polym. Sci., Polym. Phys. Ed.*, **20**, 27 (1982).
(13) D. B. Cavanaugh and C. H. Wang, *J. Appl. Phys.*, **52** (10), 5998 (1981).
(14) C. H. Wang and D. B. Cavanaugh, *Macromolecules*, **14**, 1061 (1981).
(15) D. B. Cavanaugh and C. H. Wang, *J. Appl.* Phys., **53**, 2793 (1982).
(16) D. B. Cavanaugh and C. H. Wang, *J. Polym. Sci., Polym. Phys. Ed.*, **20**, 1647 (1982).
(17) C. H. Wang, D. B. Cavanaugh, and Y. Higashigaki, *J. Polym. Sci., Polym. Phys. Ed.*, **19**, 941 (1981).
(18) J. F. Rabolt and C. H. Wang, *Macromolecules*, in press.
(19) B. A. Auld, "Acoustic Fields and Waves in Solids", Wiley, New York, 1973, Vol. 1.
(20) A. Peterlin, *J. Mater. Sci.*, **6**, 490 (1971).
(21) K. Nakayama and H. Kanetsuna, *J. Mater. Sci.*, **10**, 1105 (1975).
(22) D. B. Cavanaugh and C. H. Wang, unpublished.
(23) S. Krimm, C. Y. Liang, and G. B. B. M. Sutherland, *J. Chem. Phys.*, **25** (3), (1956).
(24) In one dimension, the wave vector K is related to δ by $\delta = 2\pi aK$, a being the length of the repeating unit.
(25) J. K. Kruger, H. Bastian, G. I. Asbach, and M. Pietralla, *Polym. Bull.*, **3**, 633 (1980).
(26) G. R. Strobl and R. Eckel, *J. Polym. Sci., Part A-2*, **14**, 913 (1976).
(27) E. W. Fischer and G. F. Schmidt, *Angew. Chem.*, **74**, 551 (1960).